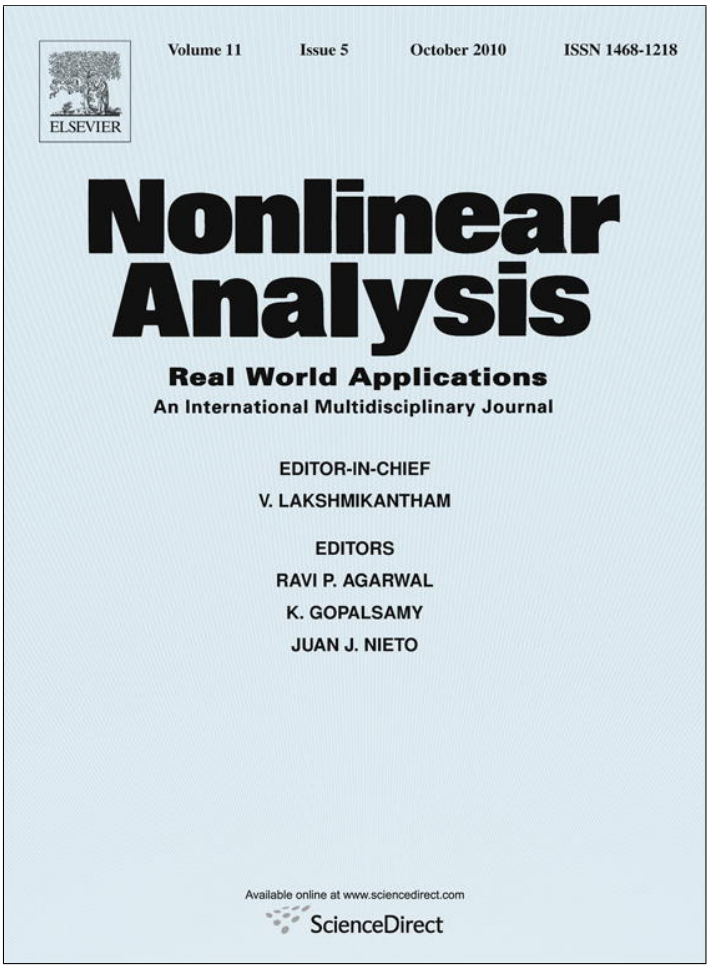

Nonlinear Analysis: Real World Applications 11 (2010) 4174–4184

Contents lists available at ScienceDirect

Nonlinear Analysis: Real World Applications

journal homepage: www.elsevier.com/locate/nonrwa

Analysis of helium bubble growth in radioactive waste

A. Carpio *, B. Tapiador

Departamento de Matemática Aplicada, Universidad Complutense de Madrid, Madrid 28040, Spain

ARTICLE INFO

Article history:
Received 25 January 2009
Accepted 1 May 2010

Keywords:
Discrete kinetic models
Integrodifferential equations
Discrete fronts
Irreversible molecular aggregation

ABSTRACT

A discrete kinetic model for the growth of helium bubbles in plutonium is proposed and analyzed. This model captures some relevant qualitative features of the time behavior of the distribution of bubble sizes. Analytic formulae for the solutions are given, which agree reasonably well with the numerical solutions, and a rigorous existence theory is established for three different equivalent formulations.

1. Introduction

Bubble growth in radioactive materials is a recently discovered phenomenon which has attracted a great deal of interest, due to its potential impact on environmental policies and energetic processes. In this paper, we focus on the growth of helium bubbles in radioactive waste (plutonium). Part of the radioactive waste generated by nuclear plants is introduced into lead containers and then buried. As time goes by, helium bubbles are generated near the walls of the containers. This phenomenon could end up damaging the walls due to the increased pressure, giving rise to radioactive pollution of the environment. Bubbles are also generated while the original radioactive paste is processed, affecting the amount of energy produced in nuclear plants. Being able to control bubble growth could result in the design of more efficient energetic procedures. However, the conditions surrounding the nucleation and growth processes in both cases are rather different.

Nucleation of bubbles in plutonium is discussed in [1,2]. As a result of alpha-decay, there is an initial transient in which auto-irradiation produces dislocations. Alpha particles become helium atoms which migrate to the holes generated during the decay. A single atom of helium is considered to be a monomer, whereas a bubble composed of k atoms is a k-cluster. Helium atoms are observed to diffuse through the medium until they find another atom, which they join forming a dimer, or a k-cluster, to form a bubble with $k+1$ atoms. These clusters do not lose atoms, due to the strong forces of attraction within them. This is an example of irreversible molecular aggregation: a cluster formed by k monomers absorbs a new monomer, but it cannot lose any of its components, in such a way that size reductions due to mass loss are impossible. Simple discrete kinetic models describe this phenomenon in different situations: colloid coagulation and fagocitosis of leukocytes [3], for instance, and the already mentioned case of bubble growth in plutonium.

A simple model for bubbles in plutonium was proposed by Schaldach and Wolfer [1]. This model considers that the initial density of helium atoms is zero, and there is a source of helium represented by a function g. The equations governing such a model are

$$\dot{\rho}_k = 4\pi D\rho_1 a_{k-1}\rho_{k-1} - 4\pi D\rho_1 a_k \rho_k, \quad k \geq 3, \tag{1}$$

$$\dot{\rho}_2 = 8\pi D\rho_1^2 a_1 - 4\pi D\rho_1\rho_2 a_2, \tag{2}$$

* Corresponding author.
E-mail address: ana_carpio@mat.ucm.es (A. Carpio).

1468-1218/$ – see front matter © 2010 Elsevier Ltd. All rights reserved.
doi:10.1016/j.nonrwa.2010.05.004

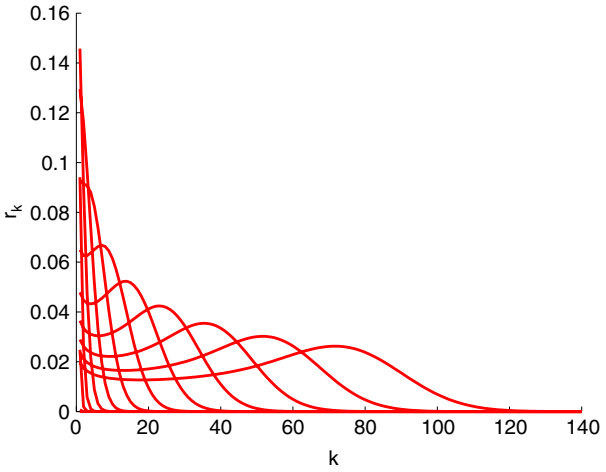

Fig. 1. Different stages of the time evolution of the distribution functions r_k as functions of the bubble size k, for model (1)–(3) with constant diffusion coefficient.

$$\rho_1 + \sum_{k=2}^{\infty} k\rho_k = \int_0^{\tilde{t}} g(t')\mathrm{d}t', \tag{3}$$

where $\dot{\rho}_k = \frac{\mathrm{d}\rho_k}{\mathrm{d}\tilde{t}}$, ρ_k being the density of k-clusters with a critical radius a_k. When the distance between the center of a k-cluster and a monomer is smaller than a_k, the monomer is absorbed and a $k+1$-cluster is created. ρ_1 represents the number of monomers by unit of volume. D is the diffusion coefficient, constant in this model. Eqs. (1) and (2) govern the rate of creation of k-mers. Eq. (3) states that the total number of atoms of helium distributed in different kinds of bubble equals the total number of atoms created by g. This model assumes that the critical radius behaves as $a_k = a_1 k^{1/3}$. For simplicity, one can set $g(t) = 1$. Nondimensionalizing, (1), (2) and (3) become

$$\frac{\mathrm{d}r_k}{\mathrm{d}t} = (k-1)^{1/3} c r_{k-1} - k^{1/3} c r_k, \quad k \geq 3, \tag{4}$$

$$\frac{\mathrm{d}r_2}{\mathrm{d}t} = 2c^2 - 2^{1/3} c r_2, \tag{5}$$

$$c = t - \sum_{k=2}^{\infty} k r_k, \tag{6}$$

with initial conditions

$$c(0) = 0, \qquad r_k(0) = 0, \quad k \geq 2. \tag{7}$$

The variable c represents the nondimensionalized density of monomers. Numerically solving this system, we compute the dimensionless distributions r_k of bubbles of size k, represented in Fig. 1. The maximum size increases without limit as time grows whereas, for each fixed size, the number of bubbles decreases. This is consistent with a constant supply of atoms. However, it fails to agree with the true observed behavior. Experimental measurements indicate two facts. First, the size of the bubbles does not grow beyond a maximum size. Second, below that maximum size, the number of bubbles of a fixed size k grows with time, being higher for a preferential value of k. The correct qualitative behavior may be achieved by adequate changes in the model; see Fig. 2.

In this paper, we slightly modify model (1)–(3) in order to reproduce the experimentally observed qualitative behavior. The idea is to replace the constant diffusion coefficient by a coefficient depending on the size of the cluster, that vanishes for large clusters. Since the bubbles are embedded in a matrix of plutonium, internal pressure should prevent large clusters from diffusing. In [4], a complex technique for 'discrete' matching was introduced to reconstruct the distribution functions for $k \geq 2$ without the need of solving the full system numerically. Here, we introduce an alternative strategy, which allows us to reconstruct the profiles without resorting to such a complex matching technique. The idea is to express the number of k-clusters as a convolution of the number of monomers with adequate kernels. Such kernels are then approximated by a family of Gaussians. The number of monomers is computed by solving a single integrodifferential equation. In this way, we obtain explicit approximate formulae for the distribution of bubbles of different size, which describe their comparative time evolution and the impact of different parameters. Comparisons with numerical solutions illustrate the value of the analytical formulae. Finally we give rigorous existence results for global solutions by combining information obtained from the original infinite system of differential equations, a reformulated version in terms of a new time variable which partially linearizes it, and the integrodifferential formulation.

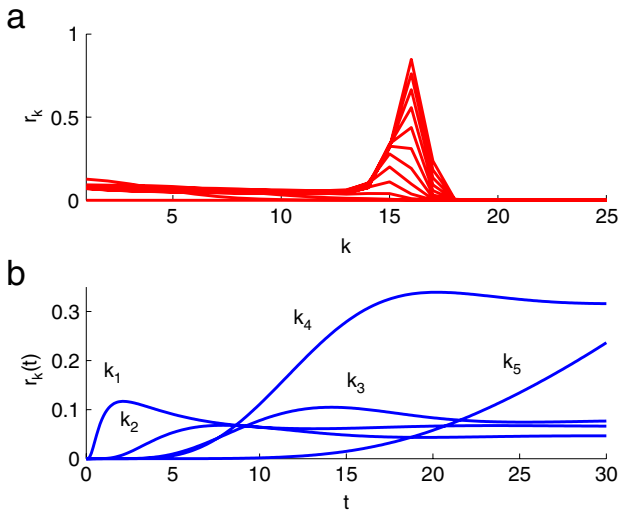

Fig. 2. (a) Different time stages of the distribution functions r_k as functions of the bubble size k. (b) Distribution functions $r_k(t)$ as functions of t, for $k_1 = 2$, $k_2 = 8$, $k_3 = 15$, $k_4 = 17$.

The rest of the paper is organized as follows. Section 2 presents the new model and some numerical results illustrating the improved qualitative behavior of the distribution of bubble sizes. In Section 3, we fit explicit formulae to the numerical solutions. Section 4 collects a few rigorous results on the existence, uniqueness and positivity of solutions. Section 5 contains our conclusions.

2. Kinetic model

Let us assume that the k-clusters diffuse according to a variable diffusion coefficient $D_0 D(k)$, $D_0 > 0$ being a constant with the correct dimensions and $D(k)$ a dimensionless function. Eqs. (1), (2) and (3) become

$$\dot{\rho}_k = 4\pi D_0 D(k-1)\rho_1 a_{k-1}\rho_{k-1} - 4\pi D_0 D(k)\rho_1 a_k \rho_k, \quad k \geq 3, \tag{8}$$

$$\dot{\rho}_2 = 8\pi D_0 D(1)\rho_1^2 a_1 - 4\pi D_0 D(2)\rho_1\rho_2 a_2, \tag{9}$$

$$\rho_1 + \sum_{k=2}^{\infty} k\rho_k = \int_0^{\tilde{t}} g(t')\mathrm{d}t'. \tag{10}$$

Nondimensionalizing, we obtain

$$\frac{\mathrm{d}r_k}{\mathrm{d}t} = (k-1)^{1/3} D(k-1) c r_{k-1} - k^{1/3} D(k) c r_k, \quad k \geq 3, \tag{11}$$

$$\frac{\mathrm{d}r_2}{\mathrm{d}t} = 2D(1)c^2 - 2^{1/3} D(2) c r_2, \tag{12}$$

$$c = t - \sum_{k=2}^{\infty} k r_k, \tag{13}$$

with zero initial conditions (7). c is again the number of monomers. Even if the initial conditions vanish, the solutions are positive due to the source term for c. This system may become stiff due to the algebraic restriction (13). For numerical purposes, it is convenient to differentiate (13) with respect to t and replace it by a differential equation for c:

$$\frac{\mathrm{d}c}{\mathrm{d}t} + 4c^2 D(1) + c M_{\frac{1}{3}} = 1, \tag{14}$$

where

$$M_{1/3} = \sum_{k=2}^{\infty} k^{1/3} D(k) r_k. \tag{15}$$

The change of variables $s = \int_0^t c(t')\mathrm{d}t'$ partially linearizes the system:

$$\frac{\mathrm{d}r_k}{\mathrm{d}s} = (k-1)^{1/3} D(k-1) r_{k-1} - k^{1/3} D(k) r_k, \quad k \geq 3, \tag{16}$$

$$\frac{dr_2}{ds} = 2cD(1) - 2^{1/3}D(2)r_2, \tag{17}$$

$$c\frac{dc}{ds} + 4c^2D(1) + cM_{\frac{1}{3}} = 1, \tag{18}$$

$$\frac{dt}{ds} = \frac{1}{c}. \tag{19}$$

Notice that the equations for $t(s)$ and $c(s)$ start from a singularity at $s = 0$. This reformulation will be used in the next section to obtain explicit formulae for the distribution of bubble sizes. This change of variables is well defined as long as $c > 0$. As we will see in Section 4, that is always the case.

Fig. 2 superimposes the distribution of bubbles sizes at different fixed times. It has been computed by solving (11)–(12) with (14) and (7). The infinite lattice is truncated to a finite size $k \leq k_0$, choosing k_0 large enough not to interact with the tail of the propagating front. For $k > k_0$, we set $r_k = 0$. This is possible because the distribution of sizes is a front advancing at finite speed. The solutions obtained with this procedure are accurate as long as the front is far enough in front of k_0. We have taken

$$D(k) = (\tanh(K_c - k) + 1)\frac{1}{2}, \tag{20}$$

where K_c is going to be a critical size. As Fig. 2(a) shows, there is a maximum bubble size. Above a certain value of k, the number of bubbles of size k is essentially zero. Below the maximum value, the number of bubbles of different sizes increases with time and a preferential size can be identified. By choosing a smaller value for K_c (about 16 here), the tail observed for $0 \leq k \leq 13$ disappears, which seem to fit better with the available histograms.

The function (20) is almost equal to one for small sizes, and then decreases abruptly to values close to zero. If we smooth out the transition, using for instance $D(k) = (\arctan(K_c - k) + \frac{\pi}{2})\frac{1}{\pi}$, the fronts do not really stop at a definite size, as we expect based on experimental evidence. Instead, near the critical size, the fronts will still advance, but very slowly. Our choice seems to reproduce the expected qualitative behavior better.

3. Integrodifferential formulation

In this section, we obtain approximate explicit expressions for the solutions of (16), (17), (18) and (19). By Laplace transforming the discrete model with respect to the variable s, the size distributions $r_k(s), k \geq 2$, are expressed as a convolution with the distribution of monomers $r_1(s) = c(s)$. The convolution kernels depend on k and are computed by inverting the Laplace transform of known functions. The structure of such kernels allows one to approximate them by either Dirac masses or a family of Gaussian-like functions. The first approximation yields an integrodifferential equation for the time evolution of the number of monomers. The second one gives reasonable approximations for the time evolution of the number of bubbles with k atoms.

3.1. Expressions for the number of k-bubbles

Laplace transforming the equations

$$\frac{dr_2}{ds} = 2cD(1) - 2^{1/3}D(2)r_2,$$

$$\frac{dr_k}{ds} = (k-1)^{1/3}D(k-1)r_{k-1} - k^{1/3}D(k)r_k, \quad k \geq 3,$$

we find

$$\hat{r}_2(\sigma) = \frac{2D(1)}{\sigma + 2^{\frac{1}{3}}D(2)}\hat{c}, \tag{21}$$

$$\hat{r}_k(\sigma) = \frac{(k-1)^{\frac{1}{3}}D(k-1)}{\sigma + k^{\frac{1}{3}}D(k)}\hat{r}_{k-1}, \quad k \geq 3. \tag{22}$$

Therefore,

$$2^{\frac{1}{3}}D(2)\hat{r}_2(\sigma) = \frac{2D(1)}{1 + \sigma 2^{\frac{-1}{3}}D(2)^{-1}}\hat{c}, \tag{23}$$

$$k^{\frac{1}{3}}D(k)\hat{r}_k(\sigma) = \frac{(k-1)^{\frac{1}{3}}D(k-1)}{1 + \sigma k^{\frac{-1}{3}}D(k)^{-1}}\hat{r}_{k-1}, \quad k \geq 3. \tag{24}$$

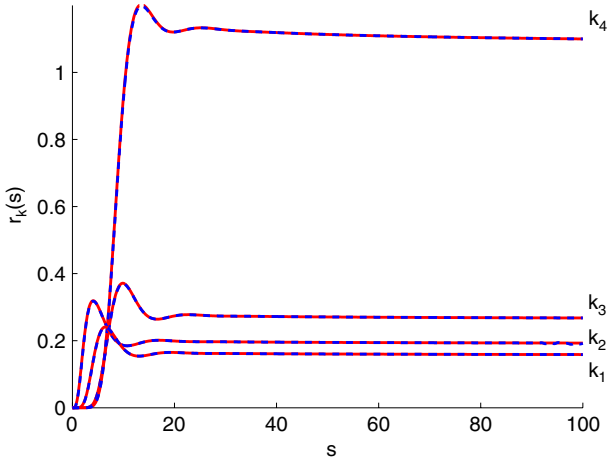

Fig. 3. Functions $r_k(s)$ for $k_1 = 12, k_2 = 15, k_3 = 18, k_4 = 21$ y $k_5 = 24$. The solid line represents the numerical solutions of the original discrete problem. The dashed line plots the approximation provided by (27), which overlaps the previous one.

By iteration,

$$k^{\frac{1}{3}} D(k)\hat{r}_k = 2\hat{c}D(1)\hat{R}_k, \tag{25}$$

where

$$\hat{R}_k(\sigma) = \prod_{j=2}^{k} \frac{1}{1 + \sigma j^{\frac{-1}{3}} D(j)^{-1}}. \tag{26}$$

Using the inversion formula

$$f(t) = \frac{1}{2\pi\imath}\int_{\mathcal{C}} \mathrm{e}^{st}\hat{f}(s)\mathrm{d}s = \frac{1}{2\pi\imath}\int_{s_1-\imath\infty}^{s_1+\imath\infty} \mathrm{e}^{st}\hat{f}(s)\mathrm{d}s,$$

in (25), we find r_k as a function of the inverse transforms R_k of $\hat{R}_k$:

$$r_k(s) = \frac{2D(1)}{k^{\frac{1}{3}} D(k)}\int_0^s R_k(s-s')c(s')\mathrm{d}s', \quad k \geq 2, \tag{27}$$

with

$$R_k(t) = \frac{1}{2\pi\imath}\int_{\mathcal{C}} \mathrm{e}^{st}\hat{R}_k(s)\mathrm{d}s = \frac{1}{2\pi\imath}\int_{s_1-\imath\infty}^{s_1+\imath\infty} \mathrm{e}^{st}\hat{R}_k(s)\mathrm{d}s = \lim_{L\to\infty}\frac{1}{2\pi}\int_{-L}^{L} \mathrm{e}^{\imath ts}\hat{R}_k(\imath s)\mathrm{d}s, \tag{28}$$

where $\mathcal{C}$ is an inversion contour. A classical choice for inversion paths is Bromwich contours $s_1 - \imath s$, parallel to the imaginary axis and located to the right of the singularities of $\hat{R}_k(s)$. In this case, we may select the imaginary axis $s_1 = 0$. For numerical purposes, the best choices of the inversion contour are those along which this inversion formula can be approximated by a quadrature formula involving a few points. We may resort instead to deformations of Bromwich contours, such as Talbot paths or hyperbolic paths; see [5].

Fig. 3 compares the numerical solutions of the original system with those provided by formula (27) using the values of $c(s)$ obtained by solving the original discrete system. The curves are indistinguishable. The next step is to derive a closed equation for c, uncoupled from the other unknowns.

3.2. Equation for the number of monomers

Using the definition of $M_{\frac{1}{3}}$, (27) and (18), we find an integrodifferential equation for the number of monomers c with initial condition $c(0) = 0$:

$$c\frac{\mathrm{d}c}{\mathrm{d}s} + 4D(1)c^2 + 2D(1)c\int_0^s \left[\sum_{k=2}^{\infty} R_k(s-s')\right] c(s')\mathrm{d}s' = 1. \tag{29}$$

Eq. (27), together with Eq. (29), provides an exact reformulation of the system of ordinary differential equations (16), (17) and (18). The integrodifferential equation for c is exact but computationally expensive. The integral kernel takes the form of a series of inverse Laplace transforms (26), (28) which have to be calculated numerically. The computational cost can be

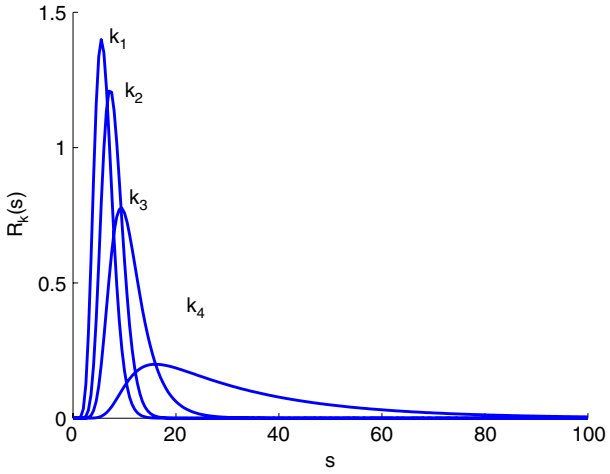

Fig. 4. Kernels R_k, for $k_1 = 12, k_2 = 15, k_3 = 18, k_4 = 21$.

reduced by conveniently approximating the kernels R_k. Fig. 4 suggests that the functions R_k can be crudely approximated by delta functions centered about their mean value $a(k) = \int_0^k \frac{\mathrm{d}s}{s^{\frac{1}{3}} D(s)}$, at least for small k.

Replacing $R_k(s - s')$ by $\delta(s - a(k))$ in (29), we get

$$c\frac{\mathrm{d}c}{\mathrm{d}s} + 4c^2 D(1) + 2D(1)c\sum_{k=2}^{\infty} c(s - a(k)) = 1.$$

If we further approximate the series by an integral and perform the change of variables $s' = s - a(k)$, $k = a^{-1}(s - s')$, $\mathrm{d}k = -(a^{-1})'(s - s')\mathrm{d}s'$, the integrodifferential equation simplifies to

$$c\frac{\mathrm{d}c}{\mathrm{d}s} + 4c^2 D(1) + 2D(1)c\int_0^s (a^{-1}(s - s'))^{1/3} D(a^{-1}(s - s'))c(s')\mathrm{d}s' = 1, \tag{30}$$

with $c(0) = 0$. This problem presents a singularity at $s = 0$, which is removed by coming back to the original time variable t:

$$\frac{\mathrm{d}c}{\mathrm{d}t} + 2cD(1)\left(2c + \int_0^t (a^{-1}(s(t) - s(t')))^{1/3} D(a^{-1}(s(t) - s(t')))[c(t')]^2 \mathrm{d}t'\right) = 1, \tag{31}$$

$$\frac{\mathrm{d}s}{\mathrm{d}t} = c. \tag{32}$$

Fig. 5 compares the values of c provided by the original discrete system and our approximated integrodifferential formulation (31)–(32). This integrodifferential system is solved by a simple scheme that combines the explicit Euler method with the composite trapezoidal rule. Even if the approximation of the kernels by delta functions was crude, especially for large k, the prediction of c provided by the resulting equation is acceptable.

Replacing R_k by $\delta(s - a(k))$ in the equations for r_k, we obtain

$$r_k(s) = \frac{2D(1)}{k^{\frac{1}{3}} D(k)}\int_0^s \delta(s - s' - a(k))c(s')\mathrm{d}s' = \frac{2D(1)}{k^{\frac{1}{3}} D(k)} c(s - a(k))\theta(s - a(k)). \tag{33}$$

However, the profiles provided by these expressions are a poor approximation of the true profiles. By choosing a less crude approximation for R_k, the results improve, as we will see in the next section.

3.3. Time evolution of the number of bubbles with k atoms

Approximating the kernels R_k by delta functions yields reasonable profiles for the density of monomers c. For the number of k-bubbles, r_k, we resort to a more precise approximation in the form of exponential kernels:

$$R(k, s) = \frac{\mathrm{e}^{\frac{-(\beta s - e(k))^2}{4\alpha(k)k}}}{(4\pi\alpha(k)k)^{\frac{1}{2}}}, \tag{34}$$

where $\beta = \frac{1}{6}$. Choosing

$$e(k) = 0.005622a(k)^2 - 0.007263a(k) + 0.836313,$$
$$\alpha(k) = 0.0491k^2 - 1.5175k + 11.7187,$$

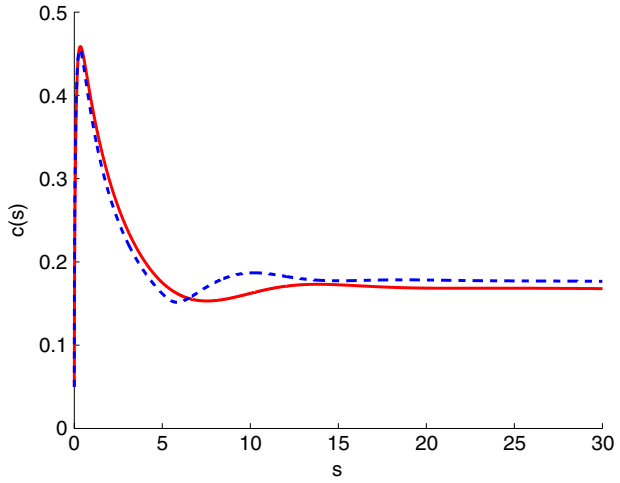

Fig. 5. Comparison of the profiles of c computed from the original discrete system (solid line) and Eq. (30) (dashed line).

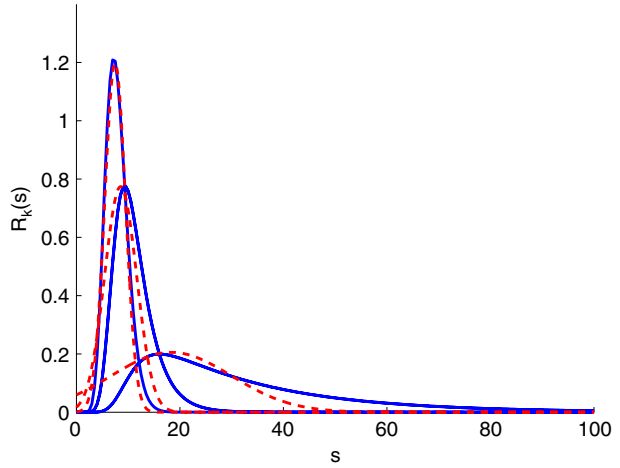

Fig. 6. Comparison between the kernels R_k and their exponential approximations. As k decreases the quality of the approximation improves.

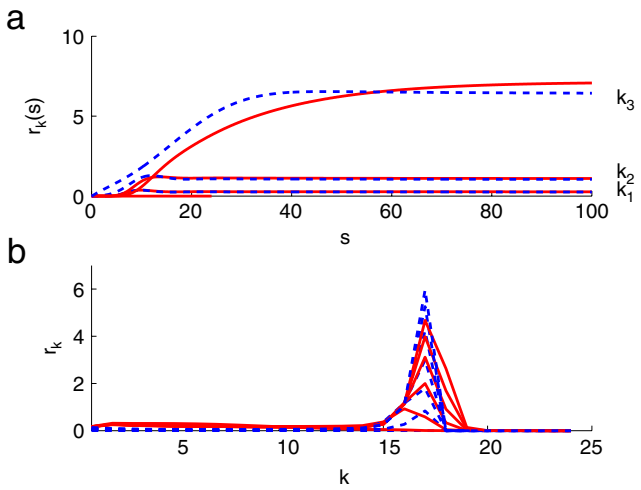

Fig. 7. (a) Number of k-bubbles $r_k(s)$ as a function of time for $k_1 = 19, k_2 = 21, k_3 = 23$. (b) Number of k-bubbles as a function of the bubble size k. Solid lines correspond to the solutions of the original discrete problem. Dashed lines represent the approximation obtained by taking Laplace transforms and approximating the kernels by exponential functions.

the resulting Gaussians approximate the kernels R_k reasonably well, especially for small and moderate k, as we can see in Fig. 6. Fig. 7 compares the true profiles r_k with those obtained using (27) and (34).

4. Well-posedness of discrete and integrodifferential problems

In this section, we prove the existence of a unique global solution for

$$\frac{dr_k}{dt} = (k-1)^{\frac{1}{3}} D(k-1) r_1 r_{k-1} - k^{\frac{1}{3}} D(k) r_1 r_k, \quad k \geq 3, \tag{35}$$

$$\frac{dr_2}{dt} = 2D(1) r_1^2 - 2^{\frac{1}{3}} D(2) r_1 r_2, \tag{36}$$

$$r_1 + \sum_{k=2}^{\infty} k r_k = \int_0^{\tilde{t}} g(t')dt' = t. \tag{37}$$

Equivalently, we may replace (37) by

$$\frac{dr_1}{dt} = 1 - 4D(1) r_1 r_1 - \sum_{k=3}^{\infty} k^{\frac{1}{3}} D(k) r_1 r_k. \tag{38}$$

The local existence of a unique solution follows using the basic theory of infinite-dimensional systems of ordinary differential equations in adequate Banach spaces. The integrodifferential equation for $c = r_1$ allows one to prove positivity: $c > 0$ as long as it exists. This ensures that the change of variables from t to s is well defined for all $t > 0$ and $s > 0$. Reformulating the discrete system in the variable s, we obtain global existence.

4.1. Local existence

Let us rewrite (35), (36) and (38) as an ordinary differential equation in the Banach space $X = \ell^\infty$ of bounded sequences:

$$Y' = F(t, Y), \qquad Y(t_0) = Y_0$$

with $Y = (r_1, \ldots, r_k, \ldots)^T$, $t_0 = 0$, $Y_0 = 0$ and $F(t, Y) = r_1 AY + G(t)$, where

$$A = \begin{pmatrix} -4D(1) & -2^{\frac{1}{3}}D(2) & -3^{\frac{1}{3}}D(3) & . & -k^{\frac{1}{3}}D(k) & . & . \\ 2D(1) & -2^{\frac{1}{3}}D(2) & 0 & . & 0 & . & . \\ 0 & 2^{\frac{1}{3}}D(2) & -3^{\frac{1}{3}}D(3) & . & . & . & . \\ . & . & . & . & . & . & . \\ . & . & . & . & . & . & . \\ . & . & . & . & 0 & . & . \\ 0 & . & 0 & (k-1)^{\frac{1}{3}}D(k-1) & -k^{\frac{1}{3}}D(k) & . & . \\ . & . & . & . & . & . & . \\ . & . & . & . & . & . & . \\ . & . & . & . & . & . & . \end{pmatrix},$$

and $G(t) = (1, 0, \ldots, 0, \ldots)^T$. Local existence follows from the following known result.

Theorem 4.1 (*[6]*). *Let $Y_0 \in X$, for a Banach space X. Let B be a closed ball centered at Y_0 with radius $\rho > 0$. Let $F : [t_0, t_0 + \alpha] \times B \longrightarrow X$ be a continuous function satisfying*

- *$\|F(t, Y)\| \leq M$ for all $(t, Y) \in [t_0, t_0 + \alpha] \times B$.*
- *$\|F(t, Y) - F(t, Z)\| \leq g(t, \|Y - Z\|)$ when $(t, Y), (t, Z) \in (t_0, t_0 + \alpha] \times B$, and g satisfies property P1 (defined below) with $\beta = 2\rho$.*

Then, if $\eta = \min(\alpha, \frac{\rho}{M})$, the initial value problem $Y' = F(t, Y)$, $Y(t_0) = Y_0$, has a unique solution for $t \in [t_0, t_0 + \eta]$.

A continuous function $g : (t_0, t_0 + \alpha] \times [0, \beta] \longrightarrow [0, \infty)$ satisfies property P1 if

- $g(t, 0) = 0$ for all $t \in (t_0, t_0 + \alpha]$.
- For every $t_1 \in (t_0, t_0 + \alpha]$, $\chi = 0$ is the unique solution of $x' = g(t, x)$ in $(t_0, t_1]$ such that $\chi(t_0+) = 0$ and $\lim_{t \to t_0+} \frac{\chi(t)}{t - t_0} = 0$.

In our case, $Y_0 = 0$ and $F = r_1 AY + G$, as defined above. Notice that the elements of the sequence $D = (D(1), D(2), \ldots, D(k), \ldots)$ decay exponentially to zero as k tends to infinity. Thus, the coefficients of A are bounded and the function $F : [0, \alpha] \times B_{l^\infty}(0, \rho) \longrightarrow l^\infty$ is continuous. On the other hand, the Lipschitz and boundedness conditions on F are satisfied:

$$\|F(t, r_1, \ldots, r_k, \ldots)\| \leq 1 + C_0(D)\|Y\|^2 \leq 1 + C_0(D)\rho^2 = M,$$
$$\|F(t, Y) - F(t, Z)\| \leq \rho C(D)\|Y - Z\| = g(t, \|Y - Z\|),$$

for all $(t, Y), (t, Z) \in (0, \alpha) \times B_{l^\infty}(0, \rho)$. Setting $\mathrm{Max}_k\, k^{1/3} D(k) = L_1$ and $\sum_{k=2}^{\infty} k^{1/3} D(k) = L_2$, the constants $C_0(D)$ and $C(D)$ are defined as $C_0(D) = \mathrm{Max}\{4D(1) + L_2, 2D(1) + 2^{1/3}D(2), 2L_1\}$ and $C(D) = 2C_0(D)$. The function g satisfies property P1

and we can apply Theorem 4.1 to get the following result.

Theorem 4.2. *System (35), (36), (37) has a unique solution with initial conditions* $r_1(0) = c(0) = 0$ *and* $r_k(0) = 0, k \geq 2$, *defined at least for* $t \leq T$, $T = \frac{\rho}{M}$.

4.2. Positivity

The positive source in Eq. (38), together with the fact that the initial data are zero, ensures the strict positivity of $c = r_1$ for a certain time. By contradiction, let us assume that $c(t_0) = 0$ for some $t_0 > 0$. Then, (38) implies that $\frac{\mathrm{d}c}{\mathrm{d}t}(t_0) = 1$. A positive function cannot vanish when its derivative is positive. Thus, $c > 0$ for all $t > 0$. Since the kernels R_k are non-negative, (27) shows that $r_k \geq 0$ for $k > 2$. We have proved the following theorem.

Theorem 4.3. *The solution* $c = r_1$ *of (29) with* $c(0) = 0$ *and the functions* r_k *defined in (27) are non-negative when the kernels* R_k *are non-negative and the series* $\sum_{k=2}^{\infty} R_k$ *converges. Moreover,* $c > 0$ *for all* $t > 0$.

Therefore, we may introduce the change of variables $\frac{\mathrm{d}s}{\mathrm{d}t} = c(s)$, and the resulting function $s(t)$ is positive and increasing. This allows us to rewrite system (35), (36), (38) in terms of the variable s. We can then Laplace transform the problem as in Section 3 to obtain the integrodifferential equation (29) for c. Going back to the variable t:

$$\frac{\mathrm{d}c}{\mathrm{d}t} + 4D(1)c^2 + 2D(1)c \int_0^t \left[\sum_{k=2}^{\infty} R_k(s(t) - s(t'))\right] c^2(s(t'))\mathrm{d}t' = 1, \tag{39}$$

$$\frac{\mathrm{d}s}{\mathrm{d}t} = c(t), \tag{40}$$

which has the form

$$U'(t) = F(t, U(t), z(t)), \tag{41}$$

$$z(t) = \int_0^t K(t, t', U(t')), \tag{42}$$

with initial condition $U(0) = 0$, where

$$U(t) = (u_1, u_2) = (c(t), s(t)), \tag{43}$$

$$K(t, t', U(t')) = \sum_{k=2}^{\infty} R_k(u_2(t) - u_2(t'))u_1^2(t'), \tag{44}$$

$$F(t, U(t), z(t)) = (F_1, F_2) = (1 - 4D(1)u_1^2(t) + 2D(1)u_1(t)z(t), u_1(t)). \tag{45}$$

Rewriting (41) as

$$U(t) = \int_0^t F(t', U(t'), z(t'))\mathrm{d}t',$$

we find an integral system of Volterra type:

$$V(t) = \int_0^t G(t, t', V(t'))\mathrm{d}t', \tag{46}$$

$$V(t_0) = V_0, \tag{47}$$

where

$$V(t) = (u_1(t), u_2(t), z(t)), \tag{48}$$

$$G(t, t', V(t')) = (G_1, G_2, G_3) = (F_1(t, V), F_2(t, V), K(t, t', V)). \tag{49}$$

Existence and uniqueness results of local solutions for such problems can also be given following [7–9]. In particular, we may apply the following result.

Theorem 4.4 (*[7]*). *Let us consider the integral equation*

$$x(t) = f(t) + \int_0^t g(t, t', x(t'))\mathrm{d}t', \quad t \in [t_0, t_0 + \alpha].$$

Under the hypotheses

(1) $f : [t_0, t_0 + \alpha] \to \mathbb{R}^n$ *is a continuous function,*
(2) $g : \Delta \times B_r \to \mathbb{R}^n$ *is a continuous function, with* $\Delta = (t, t')/t_0 \leq t' \leq t_0 + \alpha$ *and* $B_r = B(0, r)$,

(3) $g(t, t', x)$ *is locally Lipschitz with respect to* x,
(4) *if* $\beta = \sup_{t\in[t_0,t_0+\alpha]} |f(t)|$, *then* $\beta < r$,

this integral equation has a unique solution in the interval $[t_0, t_0 + \delta]$. *Moreover, this solution can be constructed as the limit of successive approximations.*

In our case, $f(t) = 0$; thus (1) and (4) are trivially true. On the other hand, $G(t, t', V(t'))$ is continuous and (2) holds. This function has continuous partial derivatives, which implies (3). As a consequence, the following theorem holds.

Theorem 4.5. *The integrodifferential equation (29) has a unique solution. Moreover, defining the sequence* $V_0 = 0$, $V_m = \int_0^t G(t, t', V_{m-1})\mathrm{d}t'$, $m \geq 1$, *we have* $V(t) = \lim_{m\to\infty} V_m(t)$.

4.3. Global existence

Once we have established the local existence of solutions and the positivity of c, the global existence follows by studying the partially linearized problem in the variable s. We may take as new initial data the values $r_k(s_0)$, $k = 1, 2, \ldots$ at a time s_0 at which $c(s_0) = r_1(s_0) > 0$ for the system

$$\frac{\mathrm{d}r_k}{\mathrm{d}s} = (k-1)^{\frac{1}{3}} D(k-1) r_{k-1} - k^{\frac{1}{3}} D(k) r_k, \quad k \geq 3, \tag{50}$$

$$\frac{\mathrm{d}r_2}{\mathrm{d}s} = 2D(1) r_1 - 2^{\frac{1}{3}} D(2) r_2, \tag{51}$$

$$\frac{\mathrm{d}r_1}{\mathrm{d}s} = \frac{1}{r_1} - 4D(1) r_1 - \sum_{k=3}^{\infty} k^{\frac{1}{3}} D(k) r_k. \tag{52}$$

Since r_1 does not vanish for $s > 0$, we may choose $m' > 0$ such that $0 < m' < r_1(s)$ for $s_0 < s < s'$, for any s'.

By the standard theory of ordinary differential equations (see [6], for instance), a local solution can be extended up to a maximum existence time s'. There are two options. Either $s' = \infty$ (and the solution is defined globally) or $s' < \infty$ and the solution blows up at time s' (in the sense that some norm blows up).

In compact form, our problem reads

$$Y' = F(s, Y), \quad Y(s_0) = Y_0,$$

with $Y = (r_1, \ldots, r_k, \ldots)^T$, $Y_0 = Y(s_0)$ and $F(s, Y) = AY + G(s)$, where A is defined in Section 4.1 and $G(s) = (\frac{1}{r_1(s)}, 0, \ldots, 0, \ldots)^T$. We may think of this nonlinear system as a linear system with a source $\frac{1}{r_1}$. Notice that $\frac{1}{r_1(s)} \to 0$ if $r_1(s) \to \infty$ as $s \to s'$; thus $r_1(s)$ cannot blow up at a finite s' because then we would have a linear system with a bounded right-hand side and the solution (which includes r_1) should be bounded. Blow up in finite time would only be possible if r_1 vanished for positive s, but we have excluded this possibility in the previous section: $0 < \frac{1}{r_1} < \frac{1}{m'}$ if $s_0 < s < s'$. We have a linear system with a bounded source and blow up in finite time is excluded. This concludes the proof of the following result.

Theorem 4.6. *System (35), (36), (38) with zero initial data has a unique solution defined for all* $t > 0$.

5. Conclusions

We have proposed and analyzed a model for the growth of helium bubbles in plutonium that reproduces reasonably some qualitative features observed experimentally. A rigorous existence theory has been established. Explicit approximate formulae for the number of bubbles of different sizes have been given, which may help to predict the impact of different parameters in the time evolution of the number of bubbles. The precise physical mechanisms behind the introduction of the space-dependent coefficients proposed in the model to ensure the presence of a maximum size for the bubbles and a preferential size are yet to be established.

Acknowledgements

This work has been supported by Spanish Government research grant FIS2008-04921-C02-02 and Madrid Autonomous Region research grant CM-910143.

References

[1] C.M. Schaldach, W.G. Wolfer, Kinetics of helium bubble formation in nuclear and structural materials, in: M.L. Grossbeck, T.R. Allen, R.G. Lott, A.S. Kumar (Eds.), Effects of Radiation Materials: 21st Symposium, ASTM STP 1447, ASTM International, West Conshohocken, 2004.
[2] A.J. Schwartz, M.A. Wall, T.G. Zocco, W.G. Wolfer, Characterization and modelling of helium bubbles in self-irradiated plutonium alloys, Phil. Mag. 85 (2005) 479–488.
[3] A.G. McKendrick, Studies on the theory of continuous probabilities with special reference to its bearing on natural phenomena of a progressive nature, Proc. Lond. Math. Soc. 13 (1914) 401–416.
[4] L.L. Bonilla, A. Carpio, J.C. Neu, W.G. Wolfer, Kinetics of helium bubble formation in nuclear materials, Physica D 222 (2006) 131–140.
[5] A. Carpio, M.L. Rapun, Domain reconstruction by thermal measurements, J. Comput. Phys. 227 (2008) 8083–8106.
[6] T.M. Flett, Differential Analysis, Cambridge Univ. Press, Cambridge, 1980.
[7] C. Corduneanu, Integral Equations and Applications, Cambridge Univ. Press, Cambridge, 1991.
[8] P. Linz, Linear multistep methods for Volterra integro-differential equations, J. Assoc. Comput. Mach. 16 (1969) 295–301.
[9] W.L. Mocarsky, Convergence of step-by-step methods for nonlinear integro-differential equations, J. Inst. Math. Appl. 8 (1971) 235–239.